

# THREE-DIMENSIONAL ACOUSTIC ANALYSIS OF CONCENTRIC TUBE RESONATOR USING GREEN'S FUNCTION

D. Veerababu and B. Venkatesham

*Department of Mechanical and Aerospace Engineering, Indian Institute of Technology Hyderabad, India*  
email: [venkatesham@iith.ac.in](mailto:venkatesham@iith.ac.in)

A three-dimensional acoustic model is developed to characterize the performance of a concentric tube resonator by using Green's function. Green's function is expressed in terms of acoustic mode shape of the annular cavity with inner wall impedance conditions. Lumped parameter model has been used for calculating specific acoustic impedance to relate the pressures across the perforated liner portion. The acoustic domain is assumed to be rigid, except at inlet and outlet, which are the locations of piston sources. The total pressure acting on each piston is evaluated by using superposition principle of acoustic pressures developed at both inlet and outlet port locations. The transfer matrix, relating acoustic state variables at upstream and downstream ends is obtained, and transmission loss is calculated to estimate the performance of the configuration. These results have been compared with that of the numerical models developed using Finite Element Methods, and good agreement has been obtained.

Keywords: transmission loss, acoustic impedance, transfer matrix, piston analogy

---

## 1. Introduction

A concentric tube resonator (CTR) is a perforated pipe covered by an annulus cavity with acoustically rigid end-terminations. It is used widely in automotive industry especially in exhaust systems due to their broadband noise absorption characteristics and low back pressure.

Acoustic analysis of CTR was started by Sullivan et al.[1] when they obtained an analytical expression for predicting transmission loss (TL) by mode superposition principle in one-dimension. Later, in order to incorporate cross-flow and reverse-flow conditions Sullivan et al.[2] developed a segmentation approach in which the perforated portion is divided into different segments and the overall transfer matrix was obtained by successive multiplication of individual transfer matrices of each segment. Rao et al.[3] extended the decoupling approach developed by Jayaraman et al.[4] to allow different flow conditions in the perforated pipe and annulus regions.

Numerous theoretical models are developed based on flow and sound pressure level conditions for the sound absorption mechanism through the perforates. For example, Elnady et al.[5] proposed a semi-empirical expression for perforate impedance which incorporates both grazing as well as bias flow effects including orifice interactions. Recently, Chris Lawn[6] has summarized various perforate impedance models that are available in the literature.

In the present work, an equivalent model of CTR is made and solved the governing equations for the stationary and homogeneous medium in terms of velocity potential function in the frequency domain by using Green's function analysis. Total pressures at the inlet and the outlet ports are obtained from the potential functions. A three-dimensional transfer matrix is formulated from these pressures, and thence the transmission loss is calculated. A numerical model is also developed to validate the results.

## 2. Analytical model

This section describes the complete derivation of three-dimensional transfer matrix of a CTR, and calculation of TL. Assumptions that are made during the analysis are stated in the corresponding sections.

Figure 1 shows the schematic diagram of a CTR. The inlet port is located at  $z = 0$  and the outlet port is at  $z = L$ . Both the ports are axisymmetric with each other and are of the same cross-sectional area ( $\pi r_1^2$ ). The perforated pipe (pipe-1) of radius  $r_1$  is covered with annulus cavity (pipe-2) of outer radius  $r_2$  over the perforated portion of length  $L$ .

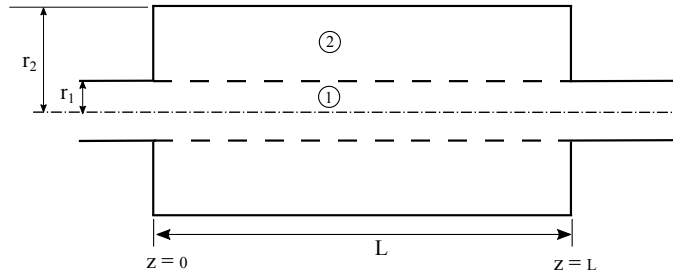


Figure 1: Schematic diagram of CTR

In the equivalent model the annulus cavity and the perforated liner are replaced with a wall of equivalent reflection coefficient  $R$  as shown in Fig 2. By doing so, the computational domain has been reduced to a uniform pipe of radius  $r_1$  with wall reflection coefficient  $R$ .

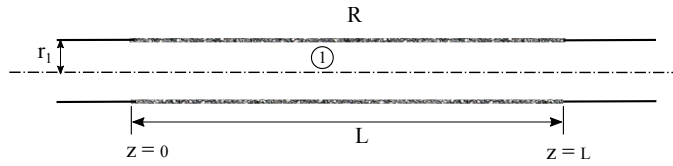


Figure 2: Equivalent model of CTR

### 2.1 Derivation of Green's function

In this analysis, it is assumed that the medium is stationary, inviscid and homogeneous with uniform density  $\rho_0$  and speed of the sound  $c_0$ . It is also assumed that the thermal conductivity of the medium and the pressure fluctuations associated with acoustic waves are sufficiently small. Under these conditions, for harmonic time dependence, the governing equation for the wave propagation in terms of the velocity potential function  $\phi(r, \theta, z)$  can be written as[7]

$$\nabla^2 \phi + k^2 \phi = 0, \quad (1)$$

and is known as homogeneous Helmholtz equation. Here  $k = \omega/c_0$  is the wavenumber and  $\omega$  is the angular frequency in rad/sec. Acoustic pressure  $p$  and particle velocity  $\mathbf{u}$  can be obtained from the potential function  $\phi$  by using the relations

$$p = -j\omega\rho_0\phi, \quad \mathbf{u} = \nabla\phi. \quad (2)$$

The velocity potential  $G(\mathbf{r}|\mathbf{r}_0)$  generated at  $\mathbf{r}$  due to a point source at  $\mathbf{r}_0$  is governed by the inhomogeneous Helmholtz equation:

$$(\nabla^2 + k^2)G(\mathbf{r}|\mathbf{r}_0) = \delta(\mathbf{r} - \mathbf{r}_0). \quad (3)$$

The function  $G$  is known as "Green's function" and  $\delta$  is the Dirac delta function. In the cylindrical coordinate system, when  $\mathbf{r} \neq \mathbf{r}_0$ , the above equation can be written as

$$\left[ \frac{1}{r} \frac{\partial}{\partial r} \left( r \frac{\partial}{\partial r} \right) + \frac{1}{r^2} \frac{\partial^2}{\partial \theta^2} + \frac{\partial^2}{\partial z^2} + k^2 \right] G(\mathbf{r}|\mathbf{r}_0) = 0. \quad (4)$$

By choosing  $G$  such that its normal derivative will vanish at the inlet and the outlet ports, and by approximating azimuthal variation with  $\cos(m\theta)$ ; the method of separation of variables yields,

$$G(\mathbf{r}|\mathbf{r}_0) = \begin{cases} AJ_m(k_r r) \cos(m\theta) \cos(k_z z) & \text{for } 0 < r < r_0, \\ B[\alpha J_m(k_r r) + Y_m(k_r r)] \cos(m\theta) \cos(k_z z) & \text{for } r_0 < r < r_1, \end{cases} \quad (5)$$

where  $A, B$  are constants and  $\alpha$  is a function related to reflection coefficient,  $R$ . The radial wavenumber ( $k_r$ ) and the axial wavenumber ( $k_z$ ) are defined as

$$k_r = \sqrt{k^2 - k_z^2}, \quad k_z = \frac{p\pi}{L}, \quad (6)$$

where  $p = 0, 1, 2, 3$ , and so on.

By integrating Eq. (3) over the domain, the required boundary conditions to determine the constants  $A$  and  $B$  can be obtained as

$$G|_{r_0+\epsilon} - G|_{r_0-\epsilon} = 0, \quad (7)$$

$$\left. \frac{dG}{dr} \right|_{r_0+\epsilon} - \left. \frac{dG}{dr} \right|_{r_0-\epsilon} = \frac{1}{r_0} \frac{\cos(m\theta_0)}{e_\theta} \frac{\cos(k_z z_0)}{e_z}, \quad (8)$$

which means  $G$  is continuous and its derivative is discontinuous at  $r = r_0$ . Here  $e_\theta$  and  $e_z$  are the normalization factors defined as

$$e_\theta = \frac{2\pi}{\epsilon_m}, \quad e_z = \frac{L}{\epsilon_p}, \quad (9)$$

where

$$\epsilon_m = \begin{cases} 1 & \text{for } m = 0, \\ 2 & \text{for } m \neq 0, \end{cases} \quad \text{and} \quad \epsilon_p = \begin{cases} 1 & \text{for } p = 0, \\ 2 & \text{for } p \neq 0. \end{cases} \quad (10)$$

Upon substituting these boundary conditions in Eq. (5), the Green's function  $G$  due to a point source at  $r = r_0$  will become

$$G(\mathbf{r}|\mathbf{r}_0) = \frac{\pi}{2} \begin{cases} \psi_1(\mathbf{r})\psi_2(\mathbf{r}_0) & \text{for } 0 < r < r_0, \\ \psi_1(\mathbf{r}_0)\psi_2(\mathbf{r}) & \text{for } r_0 < r < r_1, \end{cases} \quad (11)$$

where

$$\psi_1(\mathbf{r}) = \sum_{m=0}^{\infty} \sum_{p=0}^{\infty} \frac{1}{e_\theta e_z} J_m(k_r r) \cos(m\theta) \cos(k_z z), \quad (12)$$

$$\psi_2(\mathbf{r}) = \sum_{m=0}^{\infty} \sum_{p=0}^{\infty} \frac{1}{e_\theta e_z} [\alpha J_m(k_r r) + Y_m(k_r r)] \cos(m\theta) \cos(k_z z). \quad (13)$$

## 2.2 Derivation of equivalent reflection coefficient

The derivation of equivalent reflection coefficient ( $R$ ) of the annulus cavity and the perforated liner will be on similar lines to the method presented by Hughes et al.[8].

Let  $p^{(1)}$  and  $p^{(2)}$  be the acoustic pressures in the regions below and above the perforated liner, respectively. From Eq. (1), Eq. (2) and Eq. (5) it can be written that

$$p^{(1)} = C_1[J_m(k_r r) + RY_m(k_r r)] \cos(m\theta) \cos(k_z z), \quad (14)$$

$$p^{(2)} = [C_2 J_m(k_r r) + C_3 Y_m(k_r r)] \cos(m\theta) \cos(k_z z), \quad (15)$$

where  $C_1$ ,  $C_2$  and  $C_3$  are constants, and can be eliminated by using acoustic rigid wall boundary condition at  $r = r_2$ , the definition of specific acoustic impedance of perforated liner, and continuity of normal velocity ( $u_r$ ) at  $r = r_1$ .

By applying these boundary conditions, we obtain

$$R = \frac{(a - b) [J_m(k_r r_1) + (k_r \zeta / j k) J'_m(k_r r_1)] - a [J_m(k_r r_1) - b Y_m(k_r r_1)]}{[J_m(k_r r_1) - b Y_m(k_r r_1)] - (a - b) [Y_m(k_r r_1) + (k_r \zeta / j k) Y'_m(k_r r_1)]}, \quad (16)$$

where

$$a = \frac{J'_m(k_r r_1)}{Y'_m(k_r r_1)}, \quad b = \frac{J'_m(k_r r_2)}{Y'_m(k_r r_2)}, \quad (17)$$

and  $\zeta$  is the normalized specific acoustic impedance defined as

$$\zeta = \frac{1}{\rho_0 c_0} \left( \frac{p^{(1)} - p^{(2)}}{u_r} \right) \Big|_{r=r_1}. \quad (18)$$

In the above analysis, it is assumed that the axial and the azimuthal wavenumbers in the annulus cavity (pipe-2) are same as that of the perforated pipe (pipe-1). It can be shown from the Eq. (11) that the equivalent reflection coefficient ( $R$ ) can be related to the function  $\alpha$  as

$$\alpha = \frac{1}{R} \quad (19)$$

## 2.3 Derivation of velocity potential

Assume that there is a hypothetical piston moving back and forth with uniform velocity  $u_1$  at the inlet and with velocity  $u_2$  at the outlet ports. The total velocity potential generated by these hypothetical pistons can be obtained from the principle of superposition since the problem is assumed to be linear.

From the Kirchhoff Helmholtz integral equation, we can find velocity potential  $\phi$  at  $\mathbf{r}$  due to the source of area  $S_0$  as

$$\phi(\mathbf{r}) = - \iint [G(\mathbf{r}|\mathbf{r}_0) \nabla \phi(\mathbf{r}_0) - \nabla G(\mathbf{r}|\mathbf{r}_0) \phi(\mathbf{r}_0)] dS_0. \quad (20)$$

Since the normal derivative of  $G$  vanishes at the inlet and the outlet ports, it can be written as

$$\phi(\mathbf{r}) = - \iint G(\mathbf{r}|\mathbf{r}_0) \nabla \phi(\mathbf{r}_0) dS_1 - \iint G(\mathbf{r}|\mathbf{r}_0) \nabla \phi(\mathbf{r}_0) dS_2, \quad (21)$$

where  $S_1$  and  $S_2$  are cross-sectional area of the inlet and the outlet ports, respectively.

The boundary condition required to evaluate the above integrals are [9, 10]:

$$\left. \frac{\partial \phi}{\partial z} \right|_{z=0} = u_1 f_1(r, \theta) = N_1(r, \theta), \quad (22)$$

$$\left. \frac{\partial \phi}{\partial z} \right|_{z=L} = u_2 f_2(r, \theta) = N_2(r, \theta), \quad (23)$$

where  $f_1$  and  $f_2$  are the functions that depend on the position of the inlet and the outlet ports, respectively. Therefore,

$$\phi(\mathbf{r}) = - \iint G(\mathbf{r}|\mathbf{r}_0) N_1(r, \theta) dS_1 - \iint G(\mathbf{r}|\mathbf{r}_0) N_2(r, \theta) dS_2 = \phi_1(\mathbf{r}) + \phi_2(\mathbf{r}), \quad (24)$$

where  $\phi_1$  is the velocity potential generated by the inlet piston, and  $\phi_2$  is for that of the outlet. For the present configuration  $f_1 = f_2 = 1$ .

## 2.4 Calculation of transmission loss

From Eq. (2) we can find the average pressure acting on the piston  $i$  due to the velocity potential generated by the piston  $j$  as given in Kim et al.[9],

$$\bar{p}_{ij} = \frac{-j\omega\rho_0}{S_i} \iint \phi_j(\mathbf{r}) dS_i = v_j E_{ij}, \quad (25)$$

$$\Rightarrow E_{ij} = \frac{-j\omega\rho_0}{S_i v_j} \iint \phi_j(\mathbf{r}) dS_i \quad (26)$$

where  $v_j = u_j S_j$  is the volume velocity. Substituting Eq. (11) and Eq. (24) into the above equation leads to

$$E_{ij} = \frac{\pi j\omega\rho_0}{2 S_i S_j} \gamma_i \chi_j, \quad (27)$$

where

$$\gamma_i = \iint \psi_1(\mathbf{r}) dS_i, \quad \chi_j = \iint \psi_2(\mathbf{r}) dS_j \quad (28)$$

It must be noted that the velocity of the outlet piston is in the opposite direction to the inlet piston.

Therefore, by using the principle of superposition the total pressure acting on the piston  $i$  can be written as

$$\bar{p}_i = \bar{p}_{ii} + \bar{p}_{ij} = v_i E_{ii} + v_j E_{ij}, \quad (29)$$

and the corresponding transfer matrix ( $T$ ) as

$$\begin{bmatrix} \bar{p}_1 \\ v_1 \end{bmatrix} = \begin{bmatrix} T_{11} & T_{12} \\ T_{21} & T_{22} \end{bmatrix} \begin{bmatrix} \bar{p}_2 \\ v_2 \end{bmatrix}. \quad (30)$$

The transmission loss (TL) is defined as the difference between the incident sound power level and the transmitted sound power level when there are no downstream reflections, and can be expressed as[11]

$$TL = 20 \log \left[ \left( \frac{Z_1}{Z_2} \right)^{\frac{1}{2}} \left| \frac{T_{11} + T_{12}/Z_1 + T_{21}Z_2 + T_{22}(Z_2/Z_1)}{2} \right| \right], \quad (31)$$

where

$$Z_1 = \frac{\rho_0 c_0}{S_1}, \quad Z_2 = \frac{\rho_0 c_0}{S_2} \quad (32)$$

are the characteristic impedance of the inlet and the outlet ports, respectively.

## 3. Numerical Model

A finite element model has been prepared by discretising the perforated pipe as well as the annulus cavity in HyperMesh[12]. Maximum element size is kept below one-sixth of the minimum wavelength present in the analysis to ensure that all the waves are captured properly throughout the frequency range of interest.

The discretised model is imported directly into the Harmonic FEM Acoustic module of LMS Virtual.Lab[13]. By applying unit normal velocity excitation at the inlet and anechoic end-termination at the outlet, the model has been solved for acoustic pressures with admittance transfer relation between the perforated pipe and the annulus cavity. Imposition of anechoic termination ensures that the total pressure at the outlet is identical to the incident component of the transmitted pressure by eliminating the reflected component.

The transmission loss is calculated by using the acoustic pressures associated with the incident pressures at the inlet and the outlet ports from the formula

$$TL = 20 \log_{10} \left| \frac{p_{in} + \rho_0 c_0 u_{in}}{2p_{out}} \right|. \quad (33)$$

## 4. Results

In this section, the transmission loss (TL) obtained from the analytical model has been compared with numerical predictions. For this purpose, a CTR with typical dimensions:  $r_1 = 20$  mm,  $r_2 = 60$  mm and  $L = 200$  mm is considered. A finite element model is prepared with the same dimensions by using tetrahedron elements with approximately 1,07,300 nodes in the entire domain.

The expression for the normalized specific acoustic impedance ( $\zeta$ ) in Eq. (16) is adopted from Sullivan et al.[1] by neglecting the resistance part as shown in Eq. (34)

$$\zeta = jk(t + 0.75d_h)/\sigma \quad (34)$$

with orifice diameter  $d_h = 4$  mm, liner thickness  $t = 1$  mm and porosity  $\sigma = 0.05$ . Properties of the medium are taken as  $\rho_0 = 1.225$  kg/m<sup>3</sup> and  $c_0 = 340$  m/s.

Figure 3 shows the comparison of TL obtained from the analytical model with that of the numerical prediction. It can be observed that there is a good agreement between the results at lower as well as higher frequencies.

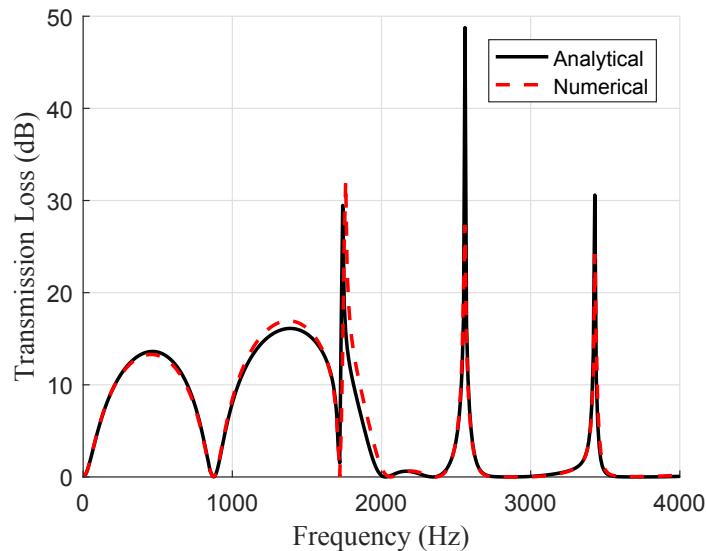


Figure 3: TL of a CTR obtained from analytical and numerical models

In the limiting value of  $\zeta \rightarrow 0$ , i.e. when the impedance offered by the perforates is negligible, the CTR configuration approaches to that of the simple expansion chamber with shell radius  $r_2$ , and the inlet and the outlet radii  $r_1$ .

It can be observed from the Fig 4 that in the limiting case of  $\zeta \rightarrow 0$  in the analytical model of CTR, the TL approaches to that of the simple expansion chamber, predicted numerically. This also assures the validity of the analysis.

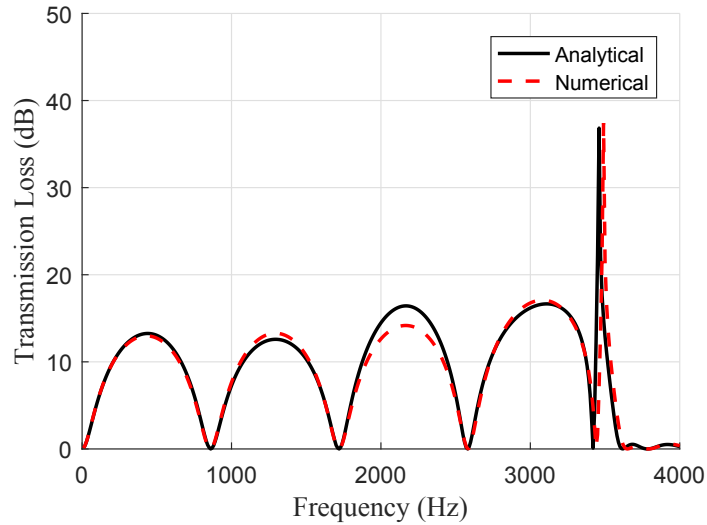


Figure 4: TL of a CTR in the limiting value of  $\zeta \rightarrow 0$  (simple expansion chamber)

It must be noted from Eq. (11) that the Green's function analysis presented here is not only applicable to a CTR but for any configuration for which the value of  $\alpha$  or the equivalent reflection coefficient ( $R$ ) can be found. In another way, it provides the means of developing three-dimensional transfer matrices for the acoustic elements such as the side branch resonator, Pod silencers, Herschel-Quincke tube, lined ducts and ducts with compliant walls etc.

Moreover, the effect of uniform mean flow can be incorporated into the analysis by changing the governing equations and thence by developing modified Green's function with the corresponding modified wavenumbers. However, it has been observed in some cases where the contribution of the resistance part becomes significant when compared with the reactance part in the normalized specific acoustic impedance expression due to the presence of flow through the orifices or due to nonlinearities associated with high sound pressure levels; the analytical model is susceptible to numerical errors.

## 5. Summary

The computational domain of CTR is reduced by an equivalent model of uniform pipe with a wall reflection coefficient. The Helmholtz equation is solved for velocity potentials with appropriate boundary conditions on the reduced model by using Green's function analysis and the expressions for four-pole parameters are obtained.

A numerical model with transfer admittance relation across the perforated liner is simulated in commercial software to validate the proposed analytical model. It is observed that good agreement has been achieved in the results. A limiting case study is conducted to further validate the methodology.

It is understood from the formulations that the analytical model presented in this work is applicable to a configuration as long as the equivalent wall reflection coefficient for that configuration is able to find. Further, it can be used under uniform flow conditions with minor fixes.

## Acknowledgements

Authors are grateful for the computational support provided by the Gas Turbine Research Establishment under GATET project.

## REFERENCES

1. Sullivan, J. W. and Crocker, M. J. Analysis of concentric-tube resonators having unpartitioned cavities, *The Journal of the Acoustical Society of America*, **64** (1), 207–215, (1978).
2. Sullivan, J. W. A method for modeling perforated tube muffler components. I. Theory, *The Journal of the Acoustical Society of America*, **66** (3), 772–778, (1979).
3. Rao, K. N. and Munjal, M. L. A generalized decoupling method for analyzing perforated element mufflers, *Proceedings of the Nelson Acoustics Conference*, Madison, Wisconsin, July, (1984).
4. Jayaraman, K. and Yam, K. Decoupling approach to modeling perforated tube muffler components, *The Journal of the Acoustical Society of America*, **69** (2), 390–396, (1981).
5. Elnady, T., Åbom, M. and Allam, S. Modeling perforates in mufflers using two-ports, *Journal of Vibration and Acoustics*, **132** (6), 1–11, (2010).
6. Lawn, C. The acoustic impedance of perforated plates under various flow conditions relating to combustion chamber liners, *Applied Acoustics*, **106**, 144–154, (2016).
7. Morse, P. M. and Ingard, K. U. Ed., *Theoretical acoustics*, Princeton university press, Princeton, NJ (1986).
8. Hughes, I. J. and Dowling, A. P. The absorption of sound by perforated linings, *Journal of Fluid Mechanics*, **218**, 299–335, (1990).
9. Kim, Y. H. and Kang, S. W. Green's solution of the acoustic wave equation for a circular expansion chamber with arbitrary locations of inlet, outlet port, and termination impedance, *The Journal of the Acoustical Society of America*, **94** (1), 473–490, (1993).
10. Venkatesham, B., Tiwari, M. and Munjal, M.L. Transmission loss analysis of rectangular expansion chamber with arbitrary location of inlet/outlet by means of Green's functions, *Journal of Sound and Vibration*, **323** (3), 1032–1044, (2009).
11. Munjal, M. L. Ed., *Acoustics of Ducts and Mufflers Second Edition*, John Wiley & Sons Inc., US (2014).
12. Altair HyperWorks 14.0, *User Manual*, Altair Engineering, Michigan, US (2016).
13. LMS Virtual.Lab Rev 13.7, *Technical Documentation*, Siemens PLM Software, Texas, US (2016).